Performance characteristics of transrectal shear wave elastography (SWE) imaging in the evaluation of clinically localised prostate cancer

Wei, Cheng; Li, Chunhui; Szewczyk-Bieda, Magdalena; Upreti, Dilip; Lang, Stephen; Huang, Zhihong

Published in:
Journal of Urology

DOI:
10.1016/j.juro.2018.03.116

Publication date:
2018

Performance characteristics of transrectal shear wave elastography (SWE) imaging in the evaluation of clinically localised prostate cancer: a prospective study

Cheng Wei[a,b], Chunhui Li[b], Magdalena Szewczyk-Bieda[c], Dilip Upreti[a], Stephen Lang[d], Zhihong Huang[b], Ghulam Nabi[a]

[a] Division of Cancer Research, School of Medicine, University of Dundee, Ninewells Hospital, Dundee DD1 9SY, UK
[b] School of Science and Engineering, University of Dundee, Dundee DD1 4HN, UK
[c] Department of Clinical Radiology, Ninewells Hospital, Dundee DD1 9SY, UK
[d] Department of Pathology, Ninewells Hospital, Dundee DD1 9SY, UK

Correspondence:

Professor Ghulam Nabi MS, MD, M Ch, FRCS (Urol)

Professor of Surgical Uro-oncology

Division of Cancer Research, School of Medicine

University of Dundee, Ninewells Hospital

Dundee

DD1 9SY

Tel: 0044 1382 5540101

E-mail: g.nabi@dundee.ac.uk

Keywords: laparoscopic radical prostatectomy; prostate cancer; shear wave elastography

This study was funded by Prostate Cancer UK (PCUK), grant number: PG12-39.

Part of this work has been accepted for presentation at AUA 2018 in San Francisco

Abstract

Objective: To test the diagnostic accuracy of SWE for the detection and phenotypic characterisation of PCa compared with whole-mount radical prostatectomy histopathology.

Materials and Methods: This was a prospective protocol-driven diagnostic accuracy study. 212 consecutive men undergoing laparoscopic radical prostatectomy (LRP) for clinically localised PCa were recruited into the study. Quantitative stiffness data of the prostate gland was obtained in each patient using an endocavitary transrectal transducer before LRP and compared with detailed histopathological examination of radical prostatectomy specimen using 3-D printing mold based technology ensuring improved image-histology orientation. Receiver operator characteristic curves (ROC) were assessed between the groups.

Results and limitations: Quantitative stiffness data estimated in kilopascals (kPa) was significantly higher in malignant compared with benign areas. With a cut-off value of 82.6 kPa, sensitivity and specificity of SWE were 96.8% and 67.8%, respectively ($p<0.05$). Significant differences were observed for different grades of cancer with Young's moduli 91.6kPa, 102.3kPa and 131.8kPa for low (Gleason score 6), intermediate (Gleason score 7) and high grade (Gleason score ≥ 8) PCa respectively ($p<0.05$). SWE also detected capsular breaches with significant prediction of PCa pathologic staging. Potential limitations include selection bias and study being single centre site.

Conclusions: Quantitative SWE via transrectal approach accurately detected cancer foci and showed significant differences between cancerous and benign tissue. Moreover, this technique can be used to reliably phenotype PCa aggressiveness.

Introduction

Prostate cancer (PCa) accounts for the second most frequently diagnosed male cancer worldwide [1, 2]. Screening studies focusing on PCa detection by prostate-specific antigen (PSA) and digital rectal examination (DRE) as primary methods demonstrate that these approaches result in unnecessary biopsies, misdiagnosis and over-treatment of patients, in particularly those with insignificant PCa [3, 4].

Patients diagnosed with localised PCa are offered either active surveillance or radical treatments. Radical treatments are invariably accompanied by high adjunct health risks and are financially costly. Particularly, patients are paying a high price for low-risk diseases. **Accurate** detection of clinically significant PCa using non-invasive imaging may allow for improved risk stratification and optimal selection of men for active surveillance, focal therapy, and/or radical therapy.

Transrectal ultrasound (TRUS) is a non-invasive imaging method. Compared with other imaging techniques such as MRI and CT, TRUS is more practical in the clinical setting with advantages of real-time, cost-effective and radiation-free [5]. Nevertheless, traditional B-mode and Doppler ultrasound images demonstrate limited sensitivity and/or specificity and have not proven to unequivocally improve diagnostic accuracy of PCa detection[6].

Malignant tissue associated with the prostate gland is stiffer compared to the surrounding benign enlargement. This is well-recognised by clinicians performing DRE. Information derived from DRE is important for the clinical decision-making process. However, independently performed DRE demonstrates poor sensitivity and specificity for assessing small and anteriorly located lesions[7].

Accordingly, with the recent introduction of TRUS shear wave elastography (SWE), it is possible to assess tissue stiffness even for non-palpable small lesions. The SWE technique is based on measurements of shear wave speed through target tissues, which can be used to dynamically map and reflect tissue stiffness (Young's modulus) properties in real time[8, 9]. Preliminary studies using SWE have been promising and suggest by implementing this technique[10], there is potential for improved cancer detection and phenotyping [11]. The technology is briefly described: shear wave pulse is generated within the target tissue by multiple focused ultrasound beams, the difference in speed of shear waves is due to the stiffness properties of propagating medium; this difference is captured by piezo-electrodes inside the transducer including all these scattered shear waves and they are plotted in a pseudo-colour-coded map with shear wave speed (m/s) or Young's modulus (kPa) in pixel overlapped with B-mode ultrasound (Figure 1).

We and others have previously reported SWE for detecting and phenotyping PCa, and demonstrated strong diagnostic performance of this methodology [11-15]. Nevertheless, to date there have been no large-scale prospective studies that have tested the diagnostic accuracy of SWE compared with radical prostatectomy histology as reference standard.

Accordingly, this prospective study aimed to:

1. Determine the diagnostic accuracy of transrectal SWE compared with the final pathology of radical prostatectomy.

2. Determine the reliability of transrectal SWE with respect to accurately characterise phenotyping various grades of PCa including establishing and validating cut-offs for benign and significant PCa.

Methods

Study population

This was a prospective protocol-driven study demonstrating prior ethical and institutional approvals (Research Ethical Committee (REC) number 13/ES/0099, Research & Development number 2012ON32) designed to assess the diagnostic accuracy of transrectal SWE ultrasound specifically for PCa. Between November 2013 and August 2017, 218 consecutive participants with clinically localized PCa opting and scheduled to LRP were recruited into the study, 6 patients were excluded because of (1) prostate specimens were sectioned and analysed by non-study pathologists (n=4) and (2) SWE data were not adequate for analysis (n=2). The basic demographic characteristics is presented in Table 1. Using previously defined criterion thresholds [16], participants were divided into low, intermediate or high risk PCa groups.

The primary outcome of the study was to determine the diagnostic accuracy of transrectal SWE for the detection and phenotyping of PCa. The secondary outcome was to determine the ability of the technology in detecting clinically significant PCa and to define risk threshold cut-off values for SWE. The presence of clinically significant PCa was defined based on a combination of Gleason grade (>6) and physical cancer burden (>5mm)[17].

Study inclusion criteria were men with confirmed PCa on TRUS guided biopsies coupled with imaging suggestive of clinically localised disease (clinically ≤T2c). Based on sample size calculated, 170 patients were required to address primary outcome. All significance calculations were two sided and based on α set at 0.05, power equal to 0.95 and effect size of 0.3. We recruited 212 men into the study to account for an estimated 20% loss of data (participant drop out, poor images, technical difficulties, etc.).

Transrectal Ultrasound SWE imaging Protocol-Index test

TRUS SWE was performed by an experienced urologist (more than 10 years of experience) on the same day of LRP for all participants using an endocavity Aixplorer® ultrasound transducer (SuperSonic Imagine, Aix-en-Provence, France) through the rectal wall focussing on the prostate avoiding any pressure on the transducer. During patient imaging, prostate glands were scanned in axial and sagittal planes from base to apex every 4~6 mm. Quantitative analyses of images were performed following examinations, imaging data of successive planes was used to construct off-line 3D images of the prostate. Participant images were then used to produce customised prostate molds, which were then used to guide slicing of the prostate following surgery.

Histopathology of radical prostatectomy as reference test

All eligible participants' prostate specimens were sectioned according to our recently published method [18]. Briefly, we applied rapid prototyping methodology using prostate images. Prostate specimens were placed in molds for sectioning to ensure orientation between histology and imaging slices [18, 19] (Figure 2-a). All prostate sections were analysed by an experienced uro-pathologist (more than 20 years of experience) without knowledge of SWE image findings. Margin status including pathological stage of the disease was defined and compared to SWE imaging.

Statistical analyses

All statistical analyses were performed using SPSS 22 (IBM Corporation, New York, US). Stiffness values of cancerous tissue and surrounding benign tissues were compared using paired Student t test. The α level was set at 0.05 to determine two-tailed significance. Receiver operator characteristic curves (ROC) were plotted for stiffness values followed by application of maximum Youden index (sensitivity-[1-specificity]), indicating sensitivity and specificity are equally important to determine optimal cut-off values between tissues that was cancerous or benign[20]. **For the purpose of cross-validation and control, ten-fold cross validation was implemented. We randomly split data into 10 subgroups with identical size, each subgroup was selected and served as a testing database while the remaining 9 subgroups were used for training. The performance was repeated for 9 additional times with different subgroups served as testing database.** Correlations between cancer stiffness and Gleason Scores (GSs) were calculated. Elasticity values representing each GS were graphed using box-and-whisker plots. Finally, tissue stiffness was correlated with histopathology outcomes to define significant PCa.

Results

Mean age of the cohort was 67.6±5.4 years with a mean PSA of 11.8±8.1 ng/ml (range 0.9 to 47). Mean prostate volume was 66.9±30.4 ml (range 20 to 207). Seven participants only had GS 6 diseases (3+3: 3%); more than half of the participants had Gleason score (GS) 7 diseases (3+4: 48% and 4+3: 17%); notably, almost one-third of participants in this series demonstrated high GS disease (3+5: 10%, 4+4: 1%, 4+5: 21%) **(Table 1**). **There were two level of analyses carried out**.

For participant-level analyses, only **averaged** index lesion scores were considered when assessing performance of SWE for low grade PCa (GS=6), intermediate PCa (GS=7) or high-grade PCa (GS≥8). This is seen in **Table 2.** Stiffness data using Young's modulus (kPa) matched with histopathology demonstrates Young's Moduli were significantly higher for high grade PCa compared with low grade disease. In the entire cohort, the median values of Young's moduli for benign, low, intermediate and high grades were 58.3kPa, 91.6kPa, 102.3kPa and 131.8kPa, respectively (**Figure 4**). **A maximum Youden index of 64.6% (sensitivity: 96.8%, specificity: 67.8%) was found with a cut-off value of 82.6kPa for SWE in being able to detect malignant versus benign tissue (p<0.05) after ten-fold cross validation (Table 3). When 82.6kPa was applied to all index lesions, AUC was 0.976 (p<0.05) (Figure 3).**

In tumour-level analyses, 509 cancer foci from total of 2544 regions (12 regions from 212 patients [**Figure 2-b**]) were marked from the whole-mount pathology. The cancer distribution map was shown in **Table 4-a**. 10.8% (55/509), 25% (127/509) and 64.2% (327/509) of cancer foci were <5mm, 5-10mm and > 10mm in size respectively. GS 3+4 was the most common cancer accounting for 58.2% (296/509) of all the cancer foci. **Table 4-b** illustrated that SWE identified cancer on the distribution map using 82.6 kPa as a cut-off value. Stiffness of the identified cancers are displayed in **Table 4-c**. As such, after considering the size of all cancers, there were no significant differences for tissue stiffness across differing sizes of cancer foci. However, the mean value of Young's modulus of GS 6 to 9 increased from 91.9kPa (GS 3+3) to 126.7kPa (GS 4+5), respectively. **The mean value for all lesions was 106.3kPa. Table 4-d showed that sensitivity for SWE to detect <5mm cancers was much lower than 5-10mm and > 10mm Cancers (30.9% vs 68.5% and 92.4%), only 9 of 32 GS6 and <5mm cancers were found by SWE.**

Figure 5 presented diagnostic results of clinically significant cancer, while demonstrating SWE outcomes for sensitivity, specificity, positive predictive value (PPV) and negative predictive value (NPV) compared with histopathology results. Sensitivity, specificity, PPV and NPV of SWE for clinically significant cancer were 88.6% (95% CI 85.1%-91.6%), 97.3% (CI 96.6-98.0%), 86.3% (CI 83.0-89.1%) and 97.8% (CI 97.2-98.3%), respectively (p<0.05).

Figure 6 is a representative figure demonstrating a 70 years old patient's ultrasound and pathology images. MRI was negative, biopsy showed GS 3+3, SWE was as high as 300kPa and suggested prostate capsular breach in peripheral area. These were all summarised in Figure 6. Prostate stones were seen in B-mode ultrasound, LRP pathology images confirmed cancer with extraprostatic extension (EPE) and GS 4+5. For the entire cohort, when pathologic stages were more aggressive, we were able to detect margins status/capsular breaches with a sensitivity and specificity of 73.9% (68/92) and 80.8% (97/120), respectively (**Table 5**, p<0.05). **All patients with capsular breach had either high grade disease (>GS 7) or large sized lesions (>10mm). When cancerous tissue size was more than 10mm and within 2mm of edge of prostate, there was 90% risk of positive surgical margin as assessed by prostate whole-mount histopathology.**

Discussion

Observations of the present study illustrated that TRUS SWE demonstrated strong diagnostic performance in clinically localised PCa. We showed that transrectal SWE could identify PCa coupled with an ability to distinguish between clinically significant and low-risk PCa. We also demonstrated that tissue stiffness measurements (Young's modulus) estimated from 12 different regions of the prostate gland using a cut-off value **(82.6kPa)** identified significant differences between benign and malignant tissue. The cut-off value was based on internal validation using ten-fold cross validation method. Particularly, we found that significant lesions (GS≥7) demonstrate higher Young's moduli compared with benign and non-significant lesions (GS≤6). Lastly, TRUS SWE also showed strong performance to predict cancer stage and status of surgical margins. These data represented a significant contribution to the body of knowledge associated with utilising transrectal B-Mode ultrasonography for screening PCa.

Despite various innovative imaging technologies aimed at improving detection and characterisation of PCa, calculating individual risk for presence of clinically significant PCa remains poor. Histology using prostate biopsies remains the gold standard for PCa diagnosis. However, TRUS guided biopsy is an invasive procedure with known risks including acute bleeding, sepsis, urinary retention and even death [21-23]. Therefore, image fusion techniques, Doppler and contrast enhanced ultrasound methods have been used to improve detection of PCa while also aiming to reduce the number of biopsies performed and minimising the occurrence of adverse events [24-27].

A number of reports, including recent guidelines have reported on the improved diagnostic performance of SWE with respect to PCa [11, 15]. However, previous studies have lacked power and used mostly grey scale based ultrasound guided biopsies as reference standard. Accordingly, there are many original features of the present study. Firstly, the present study is the largest cohort that has been used to analyse the utility of SWE in comparison to final histopathology reports from specimens using whole-mount radical prostatectomy specimens. Secondly, we confirmed that orientation involving what is observed on imaging is consistent with final histopathology slides via implementation of rapid prototyping and mold based technology [18].

In our study, we also observed that SWE showed strong diagnostic performance regarding different prostatic tissues of various regions. Cancer foci could be detected or visually colour-coded by real-time SWE scan. We demonstrated using this technique that benign tissue had an appreciably lower stiffness compared with cancer foci. **Using this advanced SWE ultrasound imaging technique, we also identified an accurate cut-off value for distinguishing suspicious cancer areas from benign prostatic tissue. Ten-fold cross validation was performed and the averaged cut-off value was 82.6kPa (Table 3). Accordingly, these observations have immediate implications for therapy and follow-up care for patients.** For example, 1) low grade PCa might not need active treatment and 2) if PCa can be reliably identified, follow-up care can be closely tracked to help in reducing mistreatment rate with high diagnostic performance and the ability of SWE to differentiate between different grades of cancer, this technology could be tested for reliable monitoring in an active surveillance cohort. **A higher cut-off compared to previous studies is due to a higher proportion of men with high grade disease. Present series also represented unscreened men for prostate cancer. It may be skewed due to the fact that most men with significant disease will opt for radical surgery as treatment option. Our cut-off value was based on robust cross-validation technique and using a better reference standard of radical prostatectomy histology.**

Positive surgical margins and extraprostatic extension of cancer may cause increased biochemical recurrence(BCR)[28]. These types of patients require extended PSA follow-up time and may also

necessitate salvage treatments after failed LRP. Therefore, preoperative testing with SWE has shown the ability to predict positive surgical margins following, while also demonstrating the potentiality to assist surgical plans and predict future adjuvant treatment.

There are several limitations of the present study. We estimated diagnostic performance of SWE in men with histopathologically confirmed PCa (selection bias). Whether similar results would also be observed in men with suspected PCa or in other screening setting needs further study. A potential learning curve associated with applying the SWE technique was not assessed and procedures were carried out by single surgeon at a single center site. Nevertheless, the robust protocol of the present study coupled with encouraging findings provide support that further research is needed in this area.

Conclusions

The TRUS SWE imaging demonstrated a high reliability and accurately distinguished PCa from benign tissues while identifying a cut-off stiffness value. Moreover, SWE technology provided a high reliability in distinguishing PCa based on their phenotypes (grades of PCa). At last, the technology has also shown good diagnostic performance in the detection of margin status and stage of the disease.

Acknowledgement

This study was funded by Prostate Cancer UK (PCUK) with grant number: PG12-39.

Word count: 2499

Figures captions

Figure 1 a: Images shows shear waves generation and plane of travel creation in two planes; b: ultrasound transducer measuring travel of shear waves and conversion of this into (c) colour-coded elastogram with red indicating high stiffness and blue representing less stiff tissue.

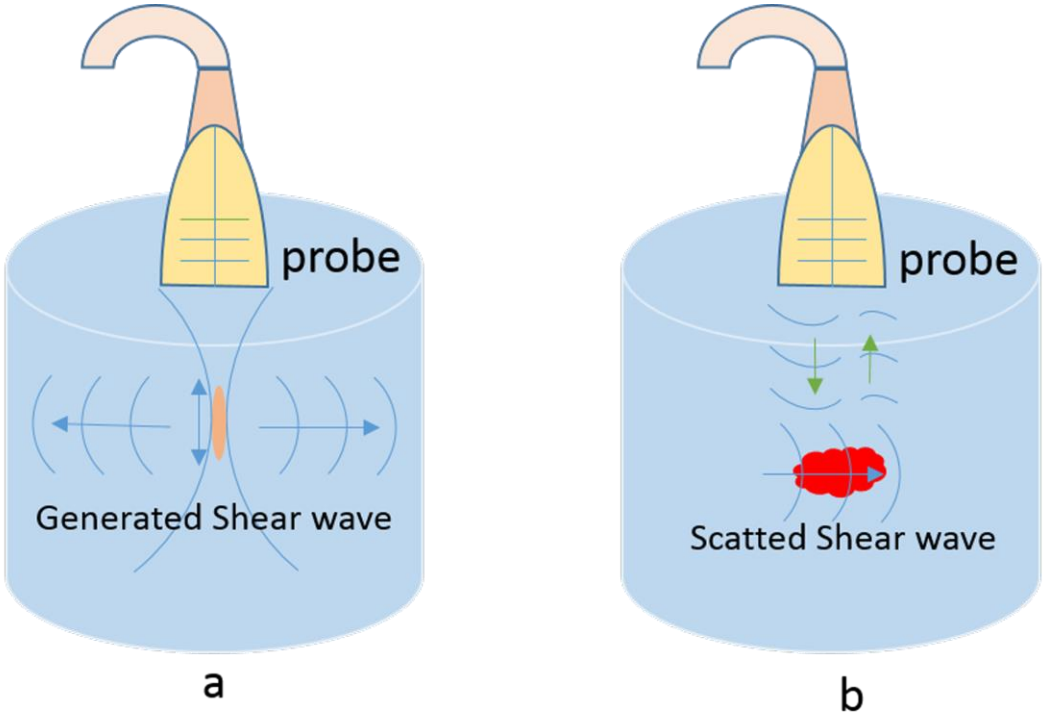

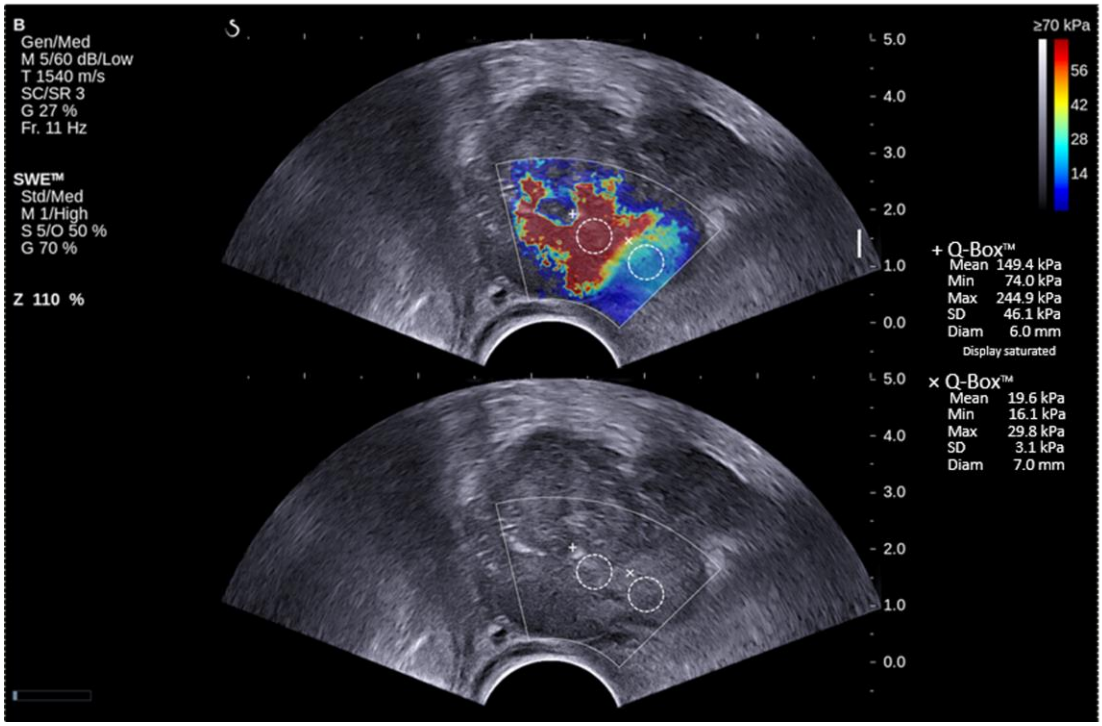

Figure 2 Comparison of histopathology results with 12- region SWE images obtained in a 73 years old patient. a: whole set of prostate slices in three locations (base, mid and apex of gland); b: 12-regions prostate imaging template; c: representative ultrasound images in apex part (Note SWE image, top; B-mode image, bottom)

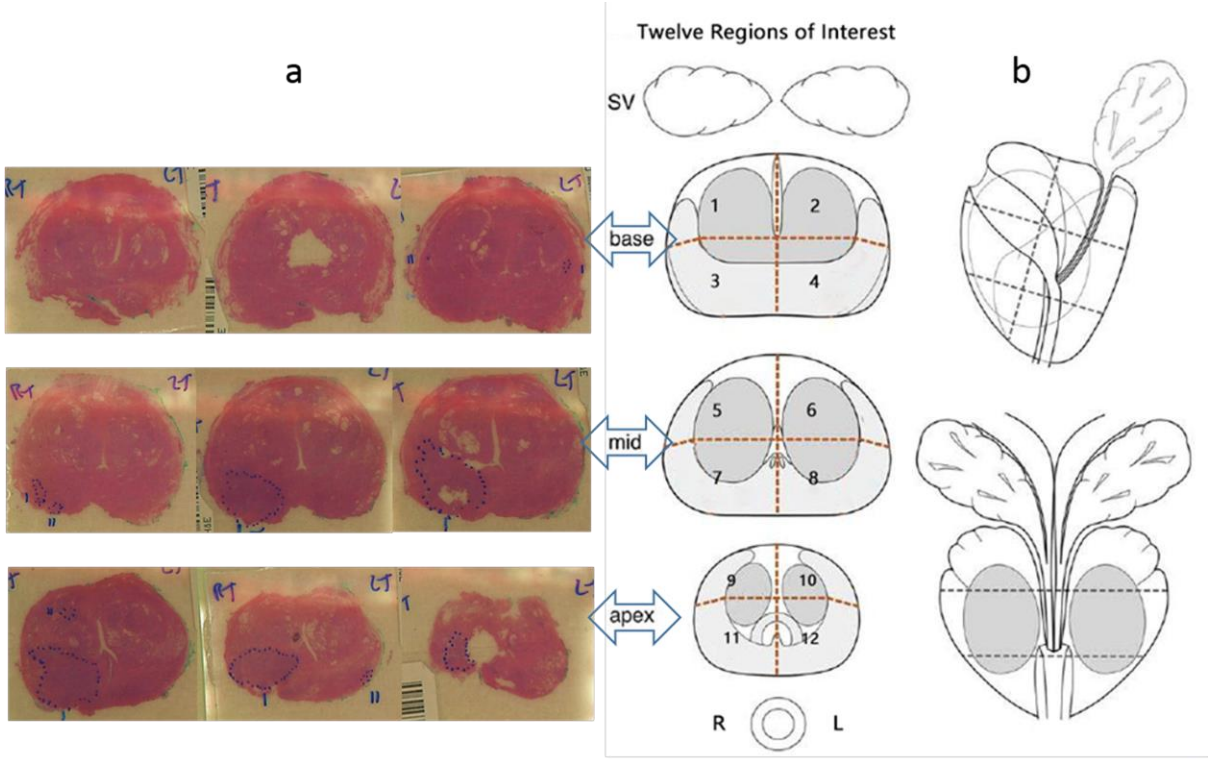

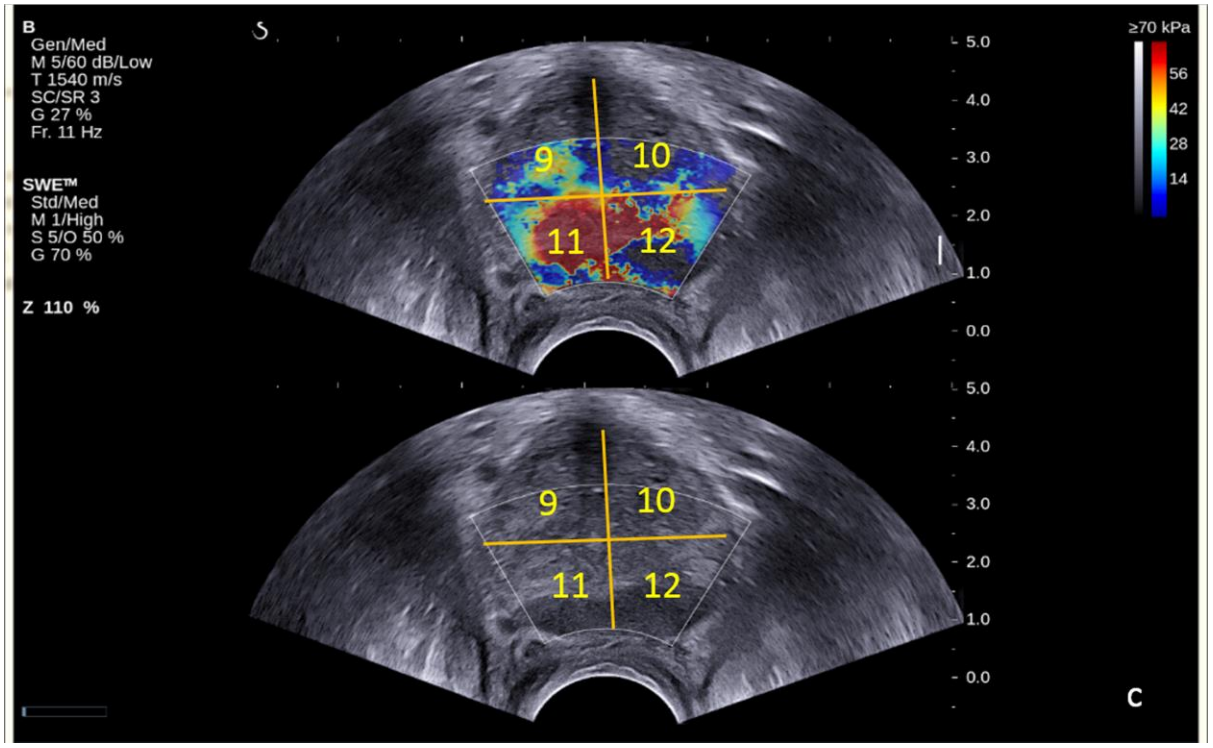

Figure 3 ROC Curve for cancer detection of prostate cancer shows an AUC of 0.97

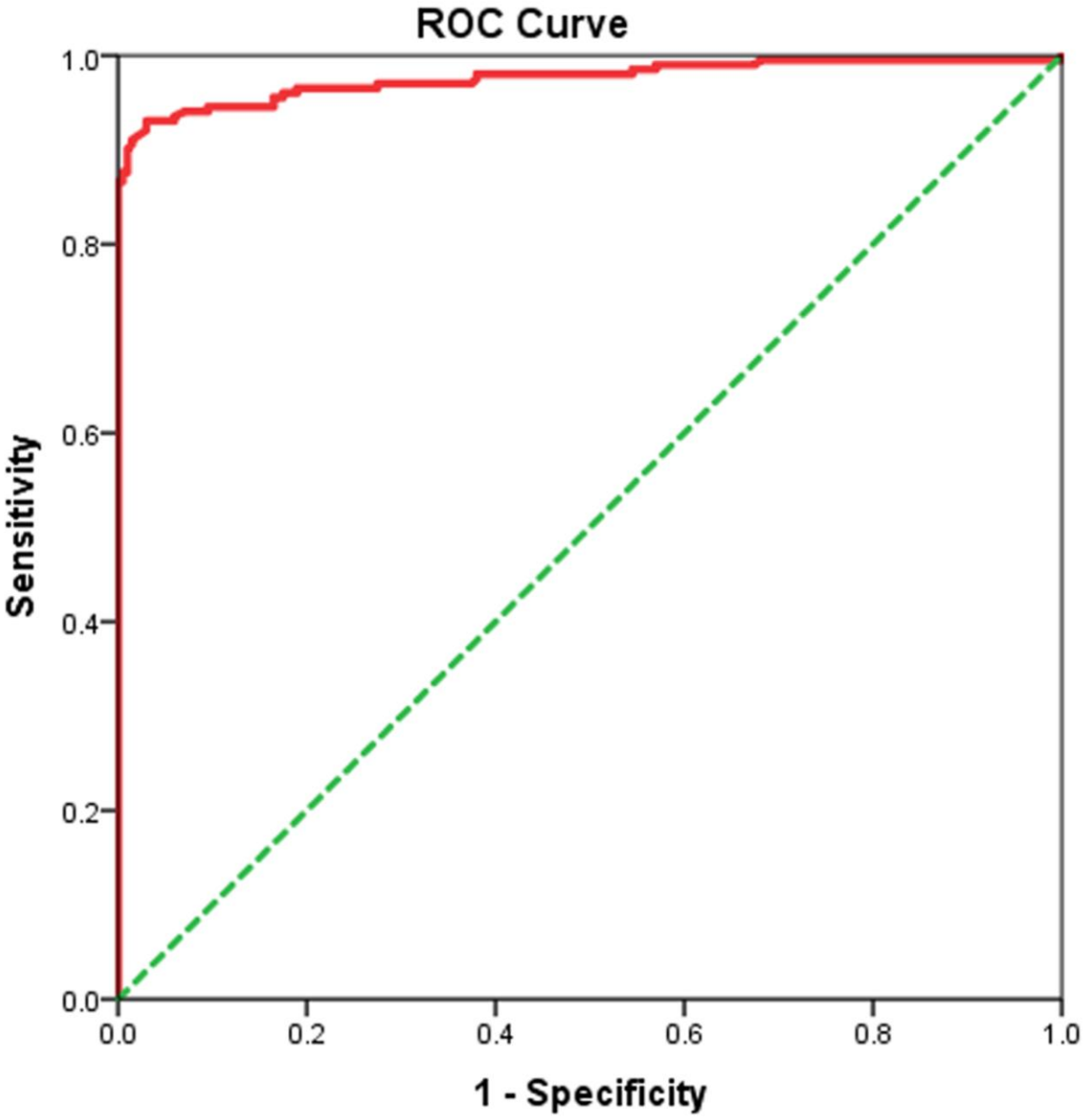

Figure 4 Box-and-whisker plot shows the tissue stiffness values of benign and different grade of malignant lesion of prostate according to the Gleason Grade

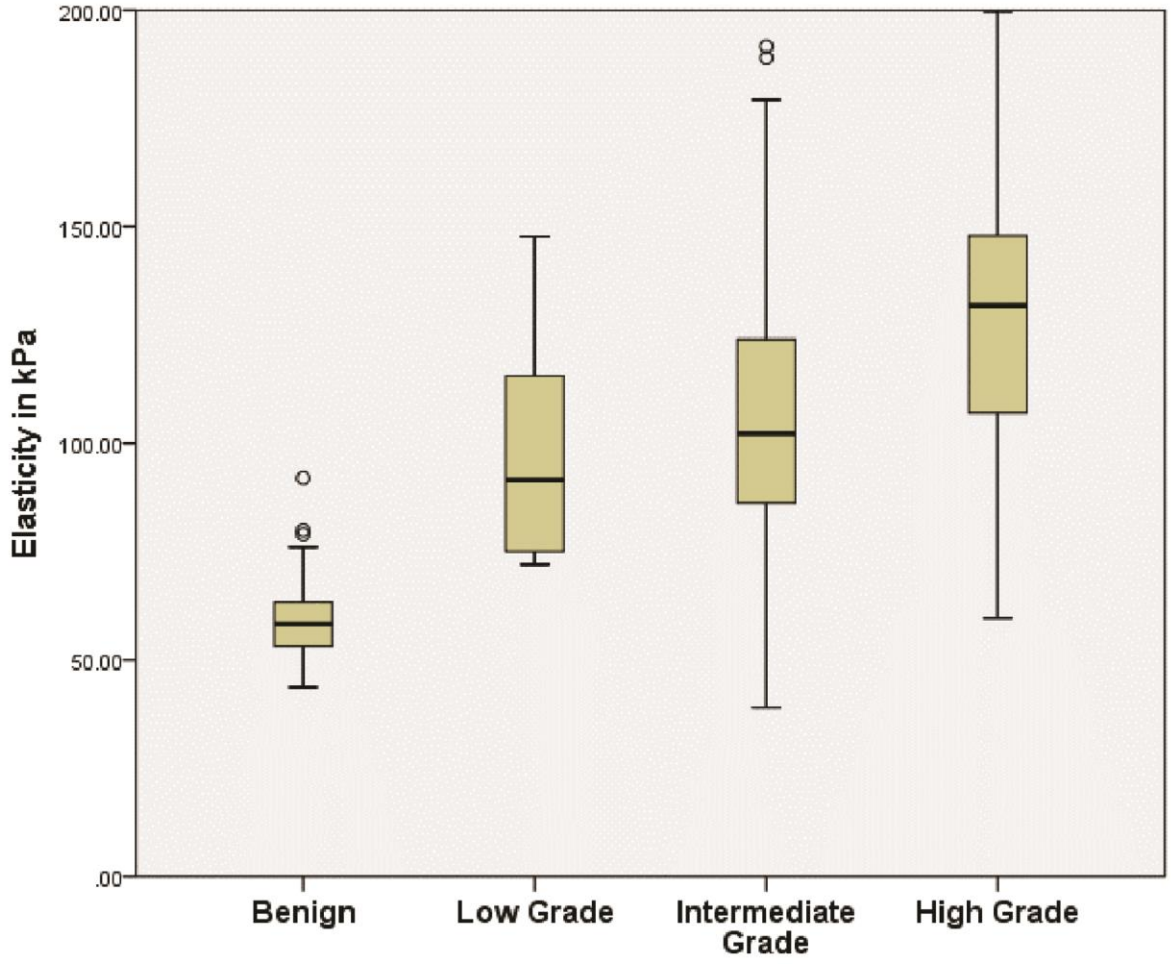

Figure 5 Diagnostic accuracy for detection of clinically significant prostate cancer (GS>6, size >5mm) on SWE imaging in comparison to reference standard test.

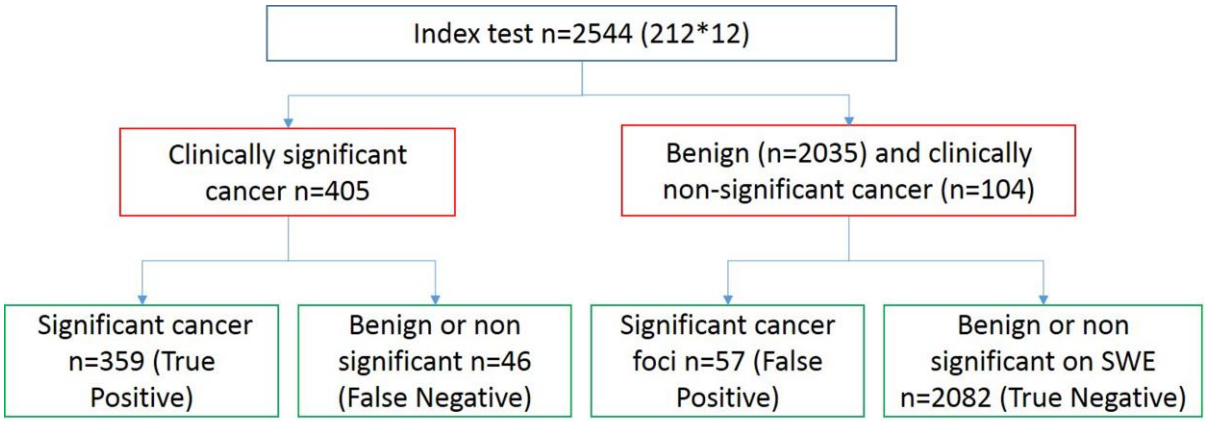

Diagnostic accuracy of SWE for significant cancers		
Sensitivity	TP/(TP+FN)	88.6% (95% CI* 85.1%-91.6%)
Specificity	TN/(TN+FP)	97.3% (95% CI 96.6-98.0%)
Positive predictive value (PPV)	TP/(TP+FP)	86.3% (95% CI 83.0-89.1%)
Negative predictive value (NPV)	TN/(TN+FN)	97.8% (95% CI 97.2-98.3%)
Accuracy (ACC)	(TP+TN)/(TP+TN+FP+FN)	96.0% (95% CI 95.1-96.7%)

: Histopathological confirmed cancer

: SWE detected cancer with cut-off 82.6kPa

* : Confident Interval

Figure 6: Illustrates an example of a 70 years old patient, MRI negative, biopsy GS 3+3, SWE shows a high tissue stiffness as 300kPa and prostate capsular breach in peripheral area (a), prostate stones show in B-mode ultrasound as hypo-intensive signal and confirm in prostate specimen slice (b), Whole-mount prostate pathology confirmed high grade cancer (GS4+5) with extraprostatic extension (EPE) pT3 disease (c).

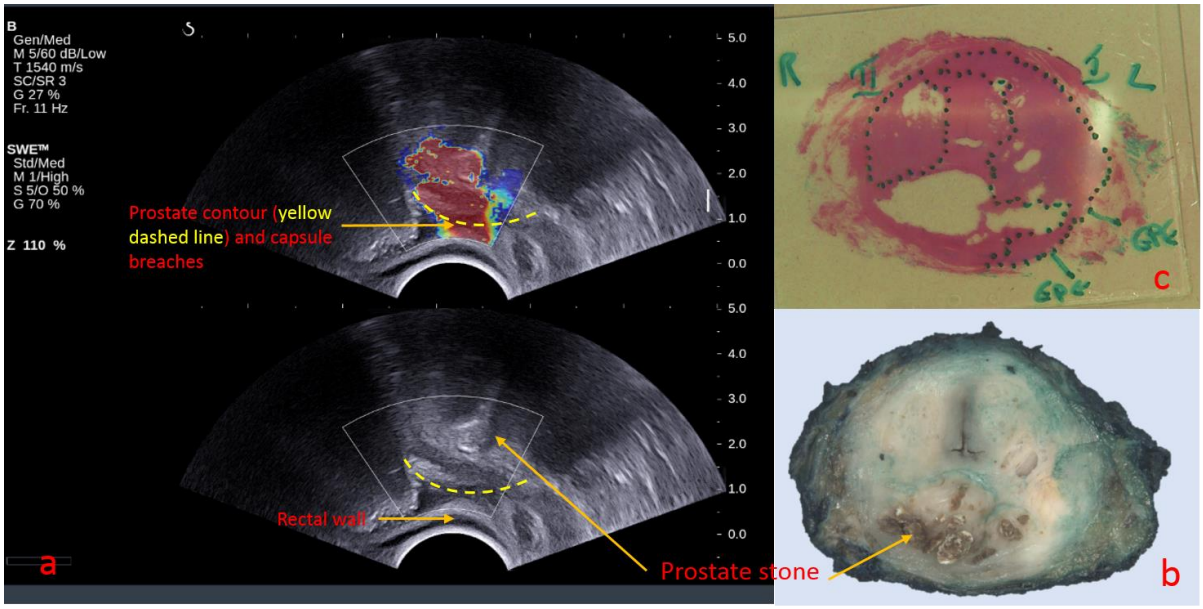

Tables captions:

Table 1 Baseline patient characteristics

Table 2 SWE-measured stiffness map of benign and cancerous lesions with various grades

Table 3: averaged AUC, cut-off value, sensitivity and specificity for SWE cancer detection from 10-fold cross validation

Table 4: Distribution map: (a) Total number of cancer foci seen on histopathology distributed by size and Gleason score; (b) SWE identified lesions out of total seen on histopathology; (c) stiffness of SWE identified lesions and (d) SWE sensitivity for different sizes and grades of cancers.

Table 5 Margin status of whole mount prostate specimens: performance of SWE (index test) in comparison to histopathology (reference test)

References

1. Mottet, N., Bastian, P.J., Bellmunt, J., et al., **Guidelines on Prostate Cancer**. European Association of Urology, 2015.
2. Torre, L. A., Bray, F., Siegel, R.L. et al, **Global cancer statistics, 2012**. CA: A Cancer Journal for Clinicians, 2015. 65(2): p. 87-108.
3. Hsing, A W., Tsao, L, and Devesa, S.S., **International trends and patterns of prostate cancer incidence and mortality**. International Journal of Cancer, 2000. 85(1): p. 60-67.
4. Loeb, S., Bjurlin, M. A., Nicholson, J., et al., **Overdiagnosis and overtreatment of prostate cancer**. Eur Urol, 2014. 65(6): p. 1046-55.
5. Spârchez, Z., **Real-time ultrasound prostate elastography. An increasing role in prostate cancer detection?** Medical Ultrasonography, 2011. 13(1): p. 3-4.
6. Harvey, C. J., Pilcher, J., Richenberg, J., et al., **Applications of transrectal ultrasound in prostate cancer**. The British Journal of Radiology, 2012. 85(Spec Iss 1): p. S3-S17.
7. Mistry, K. and Cable, G., **Meta-analysis of prostate-specific antigen and digital rectal examination as screening tests for prostate carcinoma**. J Am Board Fam Pract, 2003. 16(2): p. 95-101.
8. Bercoff, J., Tanter, M., and Fink, M., **Supersonic shear imaging: a new technique for soft tissue elasticity mapping**. IEEE transactions on ultrasonics, ferroelectrics, and frequency control, 2004. 51(4): p. 396-409.
9. Bercoff, J., Chaffai, S., Tanter, M., et al., **In vivo breast tumor detection using transient elastography**. Ultrasound in Medicine and Biology, 2003. 29(10): p. 1387-1396.
10. Rouvière, Olivier, Melodelima, Christelle, Hoang Dinh, Au, et al., **Stiffness of benign and malignant prostate tissue measured by shear-wave elastography: a preliminary study**. European Radiology, 2017. 27(5): p. 1858-1866.

11. Barr, R. G., Cosgrove, D., Brock, M., et al., **WFUMB Guidelines and Recommendations on the Clinical Use of Ultrasound Elastography: Part 5. Prostate**. Ultrasound in Medicine & Biology, 2017. 43(1): p. 27-48.
12. Ahmad, S., Cao, R., Varghese, T., et al., **Transrectal quantitative shear wave elastography in the detection and characterisation of prostate cancer**. Surgical Endoscopy and Other Interventional Techniques, 2013. 27(9): p. 3280-3287.
13. Boehm, K., Salomon, G., Beyer, B., et al., **Shear Wave Elastography for Localization of Prostate Cancer Lesions and Assessment of Elasticity Thresholds: Implications for Targeted Biopsies and Active Surveillance Protocols**. The Journal of Urology, 2015. 193(3): p. 794-800.
14. Correas, J. M., Tissier, A., Khairoune, A., et al., **Prostate Cancer: Diagnostic Performance of Real-time Shear-Wave Elastography**. Radiology, 2014: p. 140567.
15. Woo, Sungmin, Suh, Chong Hyun, Kim, Sang Youn, et al., **Shear-Wave Elastography for Detection of Prostate Cancer: A Systematic Review and Diagnostic Meta-Analysis**. American Journal of Roentgenology, 2017. 209(4): p. 806-814.
16. Muralidhar, V., Chen, M. H., Reznor, G., et al., **Definition and Validation of "Favorable High-Risk Prostate Cancer": Implications for Personalizing Treatment of Radiation-Managed Patients**. International Journal of Radiation Oncology Biology Physics, 2015. 93(4): p. 828-835.
17. Ahmed, Hashim Uddin, Hu, Yipeng, Carter, Tim, et al., **Characterizing Clinically Significant Prostate Cancer Using Template Prostate Mapping Biopsy**. The Journal of Urology, 2011. 186(2): p. 458-464.
18. Sheikh, N., Wei, C., Szewczyk-Bieda, M., et al., **Combined T2 and diffusion-weighted MR imaging with template prostate biopsies in men suspected with prostate cancer but negative transrectal ultrasound-guided biopsies**. World Journal of Urology, 2016: p. 1-8.
19. Wei, C., Lang, S., Bidaut, L., et al., **Computer aided image analysis and rapid prototyping molds using patient-specific MRI data for reliable comparison between imaging and histopathology of radical prostatectomy specimens**. British Journal of Surgery, 2014. 101: p. 67-67.
20. Fluss, R., Faraggi, D., and Reiser, B., **Estimation of the Youden Index and its Associated Cutoff Point**. Biometrical Journal, 2005. 47(4): p. 458-472.
21. Loeb, S., Vellekoop, A., Ahmed, H. U., et al., **Systematic Review of Complications of Prostate Biopsy**. European Urology, 2013. 64(6): p. 876-892.
22. Clements, R., Aideyan, O. U., Griffiths, G. J., et al., **Side effects and patient acceptability of transrectal biopsy of the prostate**. Clinical Radiology, 1993. 47(2): p. 125-126.
23. Efesoy, O., Bozlu, M., Çayan, S., et al., **Complications of transrectal ultrasound-guided 12-core prostate biopsy: a single center experience with 2049 patients**. Turkish journal of urology, 2013. 39(1): p. 6-11.
24. Ahmed, H. U., El-Shater Bosaily, A., Brown, L. C., et al., **Diagnostic accuracy of multi-parametric MRI and TRUS biopsy in prostate cancer (PROMIS): a paired validating confirmatory study**. The Lancet, 2017. 389(10071): p. 815-822.
25. Ezquer, A., Ortega Hrescak, M. C., Sanagua, C., et al., **Transrectal doppler ultrasound during prostate biopsy: Clinical utility and limitations**. Actas Urológicas Españolas (English Edition), 2015. 39(1): p. 13-19.
26. van Sloun, R. J. G., Demi, L., Postema, A. W., et al., **Ultrasound-contrast-agent dispersion and velocity imaging for prostate cancer localization**. Medical Image Analysis, 2017. 35: p. 610-619.
27. Tyson, M. D., Arora, S. S., Scarpato, K. R., et al., **Magnetic resonance-ultrasound fusion prostate biopsy in the diagnosis of prostate cancer**. Urologic Oncology: Seminars and Original Investigations, 2016. 34(7): p. 326-332.

28. Wieder, J. A. and Soloway, M. S., **INCIDENCE, ETIOLOGY, LOCATION, PREVENTION AND TREATMENT OF POSITIVE SURGICAL MARGINS AFTER RADICAL PROSTATECTOMY FOR PROSTATE CANCER**. The Journal of Urology, 1998. 160(2): p. 299-315.

Table 1. Characteristics of the cohort

Patients (N)	212
Age (LRP year)	
Median (IQR)	68 (64-72)
Mean±SD	67.6±5.4
PSA (ng/ml)	
Median (IQR)	9.4 (7.3-13.5)
Mean±SD	11.8±8.1
Prostate volume (ml)	
Median (IQR)	60 (47-76.5)
Mean±SD	66.9±30.4
Cancer volume (ml)	
Median (IQR)	20 (10-30)
Mean±SD	23.7±15.9
Gleason Score (%):	
3+3	7 (3)
3+4	101 (48)
4+3	35(17)
3+5	21 (10)
4+4	3 (1)
4+5 or more	45 (21)
pT stage (%):	
pT2a	11 (5)
pT2b	3 (1)
pT2c	106 (50)
pT3a	67 (32)
pT3b	23 (11)
pT4	2 (1)
lymph node status (%):	
pN0	187 (88)
pN1	13 (6)
pNX	12 (6)
surgical margin (%):	
Negative	120 (57)
Positive	92 (43)

Table 2: SWE-measured stiffness map of benign and cancerous lesions with various grades

Lesion Type	Min (kPa)	Max (kPa)	Mean (kPa)	SD (kPa)	Median (kPa)
benign	13.7	92.1	58.8	8.2	58.3
Low Grade (GG=6)	72	177.8	98.9	38.5	91.6
Intermediate Grade (GG=7)	69	268.2	112.1	40.2	102.3
High Grade (GG≥8)	59.7	262.5	134.5	40.3	131.8

Table 3: averaged AUC, cut-off value, sensitivity and specificity for SWE cancer detection from 10-fold cross validation

Subgroup	AUC	Cut-off value	sensitivity	specificity	P value
1	0.874	87.3	97.40%	66.40%	<0.001
2	0.877	92.5	97.20%	63.80%	<0.001
3	0.873	93.5	95.70%	68.40%	<0.001
4	0.841	91.4	100%	62.50%	0.002
5	0.876	87.3	96.70%	68.40%	<0.001
6	0.714	63.7	100%	71.40%	0.048
7	0.893	59.5	100%	66.70%	<0.001
8	0.888	92.5	95.70%	70.40%	<0.001
9	0.859	59.6	95.20%	70.20%	<0.001
10	0.864	99.1	90.30%	69.80%	<0.001
Average	0.856	82.64	96.82%	67.80%	-

Table 4: Distribution map cancer foci seen on histopathology. (a) Total number of lesions distributed by size and Gleason score (b) SWE identified lesions out of total seen on histopathology (c) stiffness of SWE identified lesions and (d) SWE sensitivity for different sizes and grades of cancers.

(a) Total cancer numbers		Size (mm)			
		<5	5~10	>10	Total
Gleason Score	3+3	32	35	14	81
	3+4	18	77	201	296
	4+3	4	12	44	60
	3+5	0	0	7	7
	4+4	0	0	4	4
	4+5 or more	3	2	58	62
	Total	55	127	327	509

(b) Number of SWE identified cancer		Size (mm)			
		<5	5~10	>10	Total
Gleason Score	3+3	9	18	12	39
	3+4	5	62	182	249
	4+3	2	5	41	48
	3+5	0	0	7	7
	4+4	0	0	4	4
	4+5 or more	1	2	56	59
	Total	17	87	302	406

(c) Stiffness of SWE identified cancer (kPa)		Size (mm)			
		<5	5~10	>10	mean
Gleason Score	3+3	88.6	87.9	100.4	90.6
	3+4	118.5	100.8	116.8	112.7
	4+3	130.3	122.5	128.3	127.2
	3+5	N/A	N/A	120.7	120.7
	4+4	N/A	N/A	153.3	153.3
	4+5 or more	85.6	160.2	167.2	165.5
	mean	102.1	100.3	126.7	120.7

(d) Sensitivity of SWE for different sizes and grades		Size (mm)			
		<5	5~10	>10	Total
Gleason Score	3+3	28.1%	51.4%	85.7%	48.1%
	3+4	27.8%	80.5%	90.5%	84.1%
	4+3	50.0%	41.7%	93.2%	80.0%
	3+5	N/A	N/A	100%	100%
	4+4	N/A	N/A	100%	100%
	4+5 or more	33.3%	100%	96.6%	95.2%
	Total	30.9%	68.5%	92.4%	79.8%

Table 5 Margin status of whole mount prostate specimens: performance of SWE (index test) in comparison to histopathology (reference test)

Margin status on pathology (reference test)		Margin status on SWE (Index test)		Total
Surgical margin	Pathology staging	Negative	Positive	
Negative	pT2a	9	0	9
	pT2b	1	2	3
	pT2c	64	12	76
	pT3a	22	6	28
	pT3b	1	3	4
	pT4	0	0	0
	Total	**97**	**23**	**120**
Positive	pT2a	2	0	2
	pT2b	0	0	0
	pT2c	5	25	30
	pT3a	10	29	39
	pT3b	7	12	19
	pT4	0	2	2
	Total	**24**	**68**	**92**
Total		**121**	**91**	**212**